frontiers in Materials

ORIGINAL RESEARCH
published: 14 May 2020
doi: 10.3389/fmats.2020.00137

Zn-Fe Double Hydroxide-Carbon Nanotube Anodes for Asymmetric Supercapacitors

*Wenyu Liang and Igor Zhitomirsky**

Department of Materials Science and Engineering, McMaster University, Hamilton, ON, Canada

Zn-Fe double hydroxide (Zn-Fe-DH) – multiwalled carbon nanotube (MWCNT) composite has been developed as a new material for energy storage in negative electrodes of asymmetric supercapacitors. A conceptually new approach is based on the use of celestine blue (CB) dye as a multifunctional additive. We discovered that CB acted as a co-dispersant for Zn-Fe-DH and MWCNT and facilitated their mixing. New strategy was based on the use of CB as charge transfer mediator, which facilitated charge-discharge reactions. The electrodes showed a capacitance of 5.2 F cm^{-2} in 0.5 M Na_2SO_4 electrolyte in a voltage window of −1.0 to −0.2 V vs. saturated calomel electrode and good cyclic stability. A new asymmetric device has been developed, containing Zn-Fe-DH-MWCNT negative electrodes and polypyrrole coated MWCNT positive electrodes. Good capacitive behavior of cathode and anode materials was achieved at high active mass of 40 mg cm^{-2} in partially overlapping potential windows. The device showed promising performance in a voltage window of 1.6 V. The capacitance of 2.2 F cm^{-2} was obtained at a scan rate of 2 mV s^{-1}.

Keywords: supercapacitor, hydroxide, zinc, iron, anode

OPEN ACCESS

Edited by:
Liang Huang,
Huazhong University of Science and Technology, China

Reviewed by:
Teng Zhai,
Nanjing University of Science and Technology, China
Liang Zhou,
Wuhan University of Technology, China
Fengjuan Chen,
Lanzhou University, China

***Correspondence:**
Igor Zhitomirsky
zhitom@mcmaster.ca

Specialty section:
This article was submitted to Energy Materials, a section of the journal Frontiers in Materials

Received: *20 February 2020*
Accepted: *21 April 2020*
Published: *14 May 2020*

Citation:
Liang W and Zhitomirsky I (2020) Zn-Fe Double Hydroxide-Carbon Nanotube Anodes for Asymmetric Supercapacitors. Front. Mater. 7:137. doi: 10.3389/fmats.2020.00137

INTRODUCTION

Transition metal-based materials have generated significant interest for applications in energy generation and storage devices (Cheong and Zhitomirsky, 2009; Zhai et al., 2018; Cesano et al., 2019; Chen et al., 2019; Dong et al., 2019). Various oxides, such as Fe_2O_3 (Nasibi et al., 2012), Mn_3O_4 (Dubal et al., 2009), MnO_2 (Su and Zhitomirsky, 2014), NiO (Chai et al., 2012), and Co_3O_4 (Xia et al., 2011) were investigated for electrodes of supercapacitors. Oxide materials showed high capacitance and good power-energy characteristics. However, due to poor electrolyte access to the active material and high electrical resistance, the specific capacitance decreases significantly with increasing active material mass. The active mass loadings for practical applications must be $\geq$ 10 mg cm^{-2} (Brisse et al., 2018).

There has been significant progress in the development of capacitive transition metal hydroxide materials. Enhanced electrochemical performance for active mass loadings of 10–28.6 mg cm^{-2} has been achieved (Chen et al., 2015; Xu et al., 2016). New techniques have been developed for the fabrication of different nanoparticles, such as nanoleafs (Xu et al., 2016), coin-like nanoplatelets (Li et al., 2011), flower-like particles (Zhang Y. et al., 2015), and nanorods (Lakshmi et al., 2014). Different $Ni(OH)_2$ phases have been investigated, such as α-$Ni(OH)_2$ (Xu et al., 2016) and β-$Ni(OH)_2$ (Li et al., 2011). New methods have been developed for the fabrication of $Ni(OH)_2$ coated carbon nanotubes (Wang et al., 2006b). Research efforts were focused on the synthesis of

nanoparticles with small particle size, high surface area, advanced design, and optimization of electrolyte composition (Xi et al., 2017). Significant interest has been generated in the development of flexible devices (Ma et al., 2016).

Various strategies have been developed for the fabrication of cobalt hydroxide and composite electrodes with active mass of 10–25 mg cm^{-2}. A hydrothermal method has been developed for the fabrication of CoOOH nanorods with a diameter of 5–10 nm (Raj et al., 2015). The nanorod nanostructure allowed for high capacitance and good cyclic stability (Raj et al., 2015). The development of advanced deposition and synthesis methods for α-$Co(OH)_2$ and β-$Co(OH)_2$ resulted in enhanced performance (Gao et al., 2013; Aghazadeh et al., 2014; Zhou et al., 2015).

There is substantial interest in investigating FeOOH and composite materials for negative electrodes. Electrochemical testing was performed in Li_2SO_4, and Na_2SO_4 electrolytes, which offer benefits for the fabrication of asymmetric devices with relatively large voltage windows (Jin et al., 2008). The columned β-FeOOH particles with diameters and lengths in the ranges of 40–50 and 200–300 nm, respectively, were prepared and used for the fabrication of electrodes (Jin et al., 2008) with mass loading of 10 mg cm^{-2}. The electrodes showed a capacitance of 116 F g^{-1} within the potential window −0.85 to −0.1 V. The high power density of 3,700 W kg^{-1} and energy density of 12 Wh kg^{-1} were achieved for an asymmetric device, containing FeOOH as a negative and MnO_2 as a positive electrode in a voltage window of 1.85 V. The development of new colloidal techniques (Silva et al., 2018) facilitated the fabrication of FeOOH and composite electrodes with active mass of 36–39.6 mg cm^{-2}. New techniques for the fabrication of non-agglomerated particles (Chen et al., 2018) allowed for enhanced performance of FeOOH electrodes. Asymmetric devices (Chen et al., 2018) containing α – FeOOH-carbon nanotube negative electrodes and MnO_2-carbon nanotube positive electrodes showed good electrochemical performance.

It was discovered that enhanced capacitive properties can be achieved in double hydroxides in KOH electrolyte. The addition of Co to $Ni(OH)_2$ resulted in the changes of microstructure (Liu et al., 2013) and a drastic improvement in the capacitance. Nanostructured Co-Si and Co-Al and Ni-Al double hydroxides were prepared with mass loadings of 20–28 mg cm^{-2}, respectively (Wang et al., 2005, 2006a, 2010; Zhang et al., 2006; Hu et al., 2013) and tested in alkaline solutions. Good electrochemical performance was achieved in hybrid Ni-Co arrays formed on a copper foam. The Ni–Co hydroxide/$Cu(OH)_2$ nanoarray exhibited ultrahigh capacitance, excellent rate capacity and good cycling stability (Zhang et al., 2016).

Previous investigations showed that the development and testing of double hydroxide materials is a promising avenue for the fabrication of advanced supercapacitor electrodes. The objective of this investigation was the development of Zn-Fe double hydroxide (Zn-Fe-DH) for negative electrodes of supercapacitors. Following this work objective, we have developed electrodes with high active mass in order to meet requirements (Brisse et al., 2018) of mass loadings ≥ 10 mg cm^{-2} for practical applications. The approach was based on the use of celestine blue dye as a multifunctional dispersant. We targeted the development of electrodes for operation in Na_2SO_4 electrolyte, which is beneficial for the development of asymmetric devices with enlarged voltage window. An asymmetric device has been fabricated and tested, containing Zn-Fe-DH negative electrodes and polypyrrole-MWCNT positive electrodes.

EXPERIMENTAL PROCEDURES

Iron chloride hexahydrate ($FeCl_3 \cdot 6H_2O$), zinc chloride ($ZnCl_2$), celestine blue (CB), sodium sulfate (Na_2SO_4), eriochrome cyanine R (ECR), pyrrole (Py), ammonium persulfate [$(NH_4)_2S_2O_8$] (APS), and poly(vinyl butyral-co-vinyl-alcohol-co-vinyl acetate) (PVB, average Mw = 50,000–80,000) were purchased from Sigma Aldrich Corp. Multi-walled carbon nanotubes (MWCNT, ID 4 nm, OD 13 nm, length 1∼2 μm) were purchased from Bayer (Germany), and Ni foams with 95% porosity were provided by Vale Canada Limited.

Synthesis of Zn-Fe-DH was performed by a chemical precipitation method, described in the literature (Krehula et al., 2006) which presents data on characterization of this material. In a typical procedure, MWCNT were added to 50 mL of

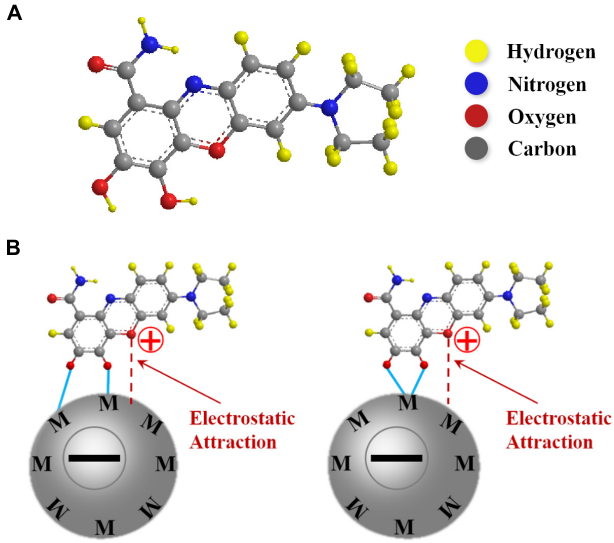

FIGURE 1 | (A) Chemical structure of CB **(B)** adsorption mechanisms of CB on metal surface by (a) bridging and (b) chelation.

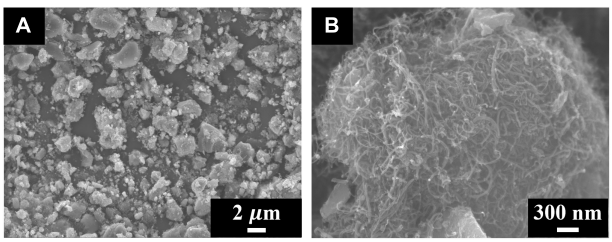

FIGURE 2 | SEM for Zn-Fe-DH -MWCNT at **(A,B)** different magnifications.

CB solution in a mass ratio 1:1 and obtained suspension was ultrasonicated for 0.5 h. $ZnCl_2$ and $FeCl_3{\cdot}6H_2O$ in a molar ratio R = [Zn]/[Zn]+[Fe] of 0.1 were dissolved in DI water. The pH of the solution was adjusted to 13.8 by dropwise addition of 4M NaOH for the precipitation of Zn-Fe-DH. Then suspensions of CB dispersed MWCNTs and Zn-Fe-DH were mixed and ultrasonicated for 45 min, followed by the filtration and drying procedure at 60°C for 24 h. The composites were mixed with PVB (3% by mass) and impregnated from a suspension in ethanol into the Ni foam current collectors. The negative electrodes were fabricated with mass loadings of 40 mg cm^{-2}.

For the synthesis of polypyrrole-coated MWCNT (PPy-MWCNT), ECR and MWCNT were mixed in 50 mL DI water in a mass ratio of 2:9, followed by ultrasonication for 30 min. The obtained MWCNT suspensions, containing ECR as a dispersant, were kept in ice bath to maintain the temperature at 4°C, and 0.24 mL of Py solution was added. Chemical polymerization of PPy was performed by addition of APS solution to the Py-MWCNT mixture, containing ECR as a dopant for PPy polymerization and dispersant for MWCNT. Obtained PPy-MWCNT contained PPy and MWCNT in a mass ratio 3:7. The reaction was carried out for 5 h. PPy-MWCNT were filtrated and dried at 60°C for 24 h. PPy-MWCNT were mixed with PVB (3% by mass) in ethanol and impregnated into the Ni foam current collectors. The positive electrodes were fabricated with mass loadings of 40 mg cm^{-2}.

Cyclic voltammetry (CV) and impedance spectroscopy (EIS) were performed using a potentiostat (PARSTAT 2273, Princeton Applied Research). The electrochemical measurements were carried out in a three-electrode setup with 0.5 M Na_2SO_4 electrolyte. Pt gauze and saturated calomel electrode (SCE) were used as counter and reference electrodes, respectively, and the area of working electrode was 1 cm^2. CV studies were performed at scan rates of 2–100 mV s^{-1}, and the gravimetric capacitance (C_m = Q/2ΔVm) and areal capacitance (C_s = Q/2ΔVA) were calculated by integrating the CV curve area (Shi and Zhitomirsky, 2010) to obtain charge Q, and subsequently dividing by the voltage window (ΔV) and mass (m) or area (A). EIS measurements were carried out in the frequency range of 10 mHz–100 kHz with a sinusoidal signal of 10 mV. The components of complex capacitance (Cs′ and Cs″) were calculated from the EIS data as $Cs' = Z''/\omega|Z|^2A$ and $Cs'' = Z'/\omega|Z|^2A$, where $\omega = 2\pi f$ and f is frequency. Galvanostatic charge-discharge of the device was performed using a battery analyzer (BST8-MA, MTI Corp.).

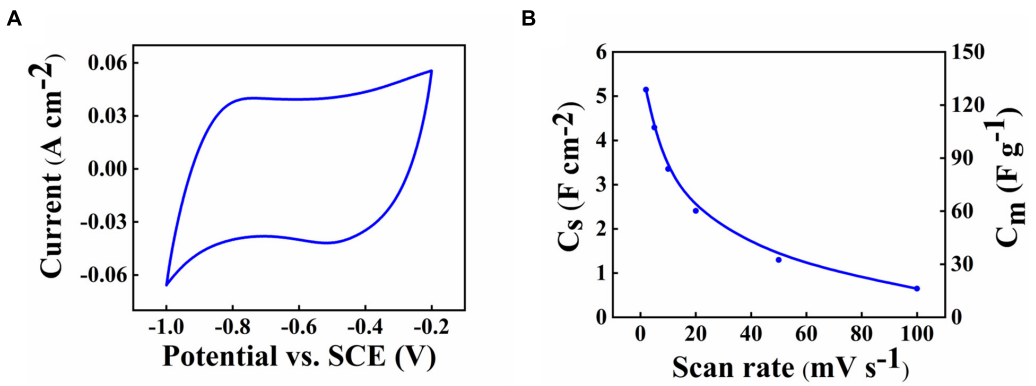

FIGURE 3 | (A) CVs at scan rate of 10 mV s^{-1} and **(B)** C_S and C_m for Zn-Fe-DH -MWCNT.

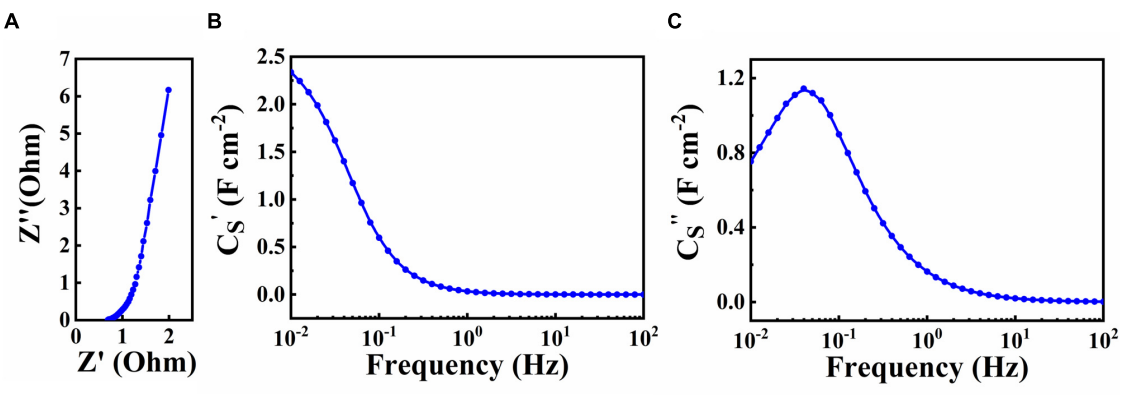

FIGURE 4 | (A) Nyquist plot of complex impedance and frequency dependences of complex capacitance components **(B)** Cs′ and **(C)** Cs″ for Zn-Fe-DH -MWCNT.

RESULTS AND DISCUSSION

Figure 1A shows chemical structure of CB, used in this investigation as a co-dispersant for MWCNT and Zn-Fe-DH. The dispersant adsorption on inorganic particles plays an important role in the particle dispersion (Wang et al., 2011). The polyaromatic structure of CB was beneficial for its adsorption on MWCNT, which involved π-π interactions (Ata et al., 2018). It should be noted that the chemical structure of CB contains a catechol group. Various molecules from catechol family showed strong adsorption on various inorganic materials (Ata et al., 2014). Similar to other catecholates, the adsorption of CB on Zn-Fe-DH involved bridging or chelating bonding (**Figure 1B**). Moreover, electrostatic interactions promoted CB adsorption on Zn-Fe hydroxide. Electrophoretic deposition experiments showed that Zn-Fe-DH particles, precipitated at pH = 13.8, were negatively charged. Therefore, the electrostatic attraction of negatively charged Zn-Fe-DH and positively charged CB facilitated CB adsorption on the Zn-Fe-DH particles. It was found that adsorbed cationic CB provided electrostatic dispersion of MWCNT and Zn-Fe-DH particles. Sedimentation tests revealed enhanced stability of MWCNT and Zn-Fe-DH suspensions, containing CB. It was hypothesized that CB can potentially improve mixing of MWCNT and Zn-Fe-DH because CB, adsorbed on the MWCNT, interacted with Zn-Fe-DH particles by chemical bonding or electrostatic interactions.

Figure 2 shows Zn-Fe-DH -MWCNT composite particles. The typical size of the particles was 0.5–3 μm (**Figure 2A**). The SEM image at higher magnification (**Figure 2B**) showed that MWCNT created a network inside the Zn-Fe-DH matrix. The conductive MWCNT matrix was beneficial for capacitive behavior.

The SEM data coupled with sedimentation tests confirm that CB provided dispersion of Zn-Fe-DH and MWCNT, which was beneficial for their enhanced mixing. The SEM images of as-received MWCNT were presented in a previous investigation (Wallar et al., 2017). As-received MWCNT formed large agglomerates with a typical size of 500 μm. It is challenging to break down such agglomerates. However, such large agglomerates were not observed in the low magnification image shown in **Figure 2A**. Therefore, CB allowed efficient dispersion of MWCNT, which formed much smaller composite particles, containing MWCNT in the Zn-Fe-DH matrix (**Figure 2B**). The Zn-Fe-DH electrode showed a nearly rectangular CV (**Figure 3**). The capacitance of 5.2 F cm^{-2} was achieved at a scan rate of 2 mV s^{-1}. The high capacitance was achieved at relatively low resistance R = Z' (**Figure 4A**). The frequency dependence of complex capacitance showed a relaxation type dispersion (**Figures 4B,C**) with relaxation frequency of about 50 mHz. EIS data indicated that the electrodes prepared using CB showed reduced resistance and higher capacitance, compared to the electrodes prepared without CB (**Supplementary Figures S1A–C**). The electrodes showed capacitance retention of 98% after 1,000 cycles (**Figure 5**). The capacitive behavior of the electrodes has also been studied by chronopotentiometry. **Figure 6** shows typical charge-discharge curves at different current densities. The charge-discharge curves at different current densities in the range of 3–10 mA cm^{-2} were of nearly triangular shape in the voltage window of −1.0 to −0.2 V. Good electrochemical performance of

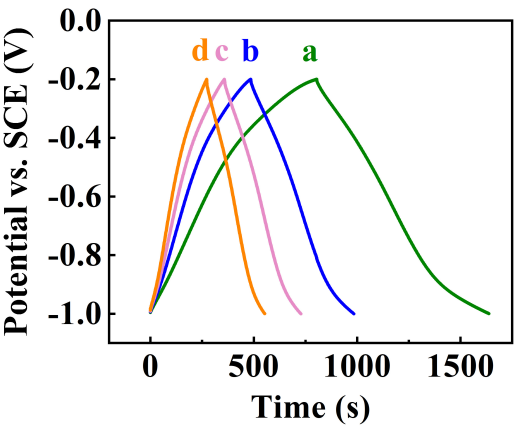

FIGURE 6 | Galvanostatic charge-discharge curves at current densities of (a) 3, (b) 5, (c) 7, (d) 10 mA cm^{-2} for Zn-Fe-DH -MWCNT.

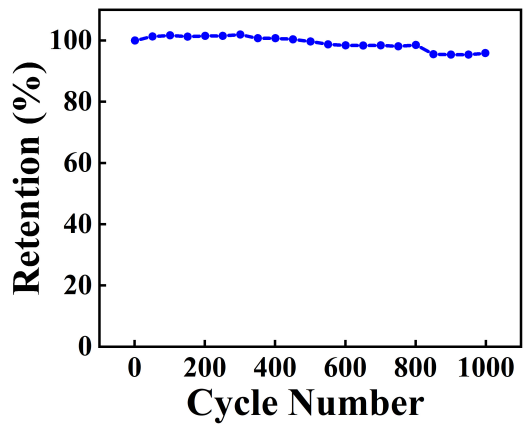

FIGURE 5 | Capacitance retention vs. cycle number for Zn-Fe-DH -MWCNT.

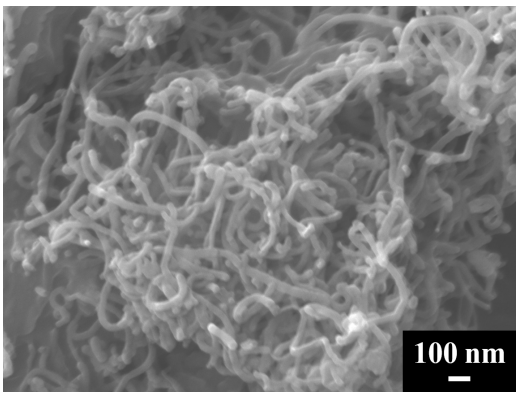

FIGURE 7 | SEM image of PPy-MWCNT composite.

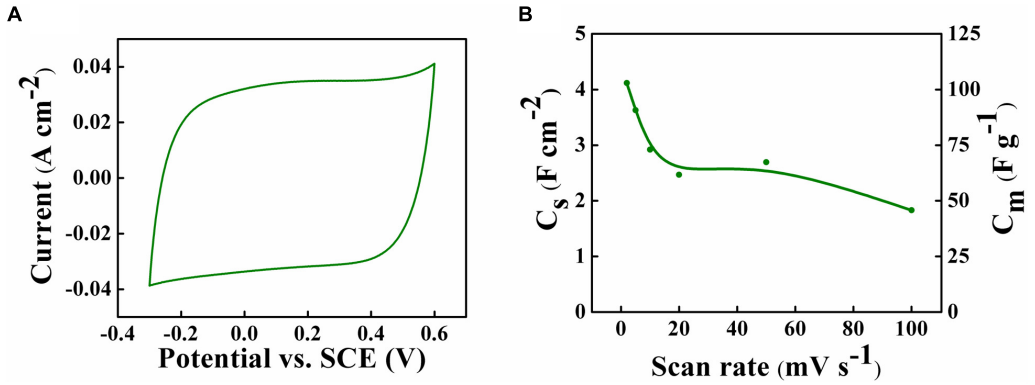

FIGURE 8 | (A) CV at scan rate of 10 mV s^{-1} and **(B)** C_s and C_m vs. scan rate for PPy-MWCNT composite.

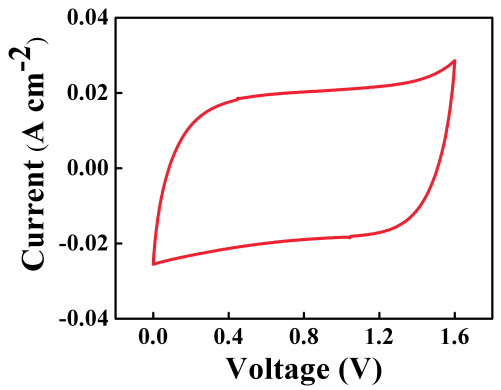

FIGURE 9 | CV at scan rate of 10 mV s^{-1} of asymmetric supercapacitor cell containing Zn-Fe-DH -MWCNT negative electrode and PPy-MWCNT positive electrode.

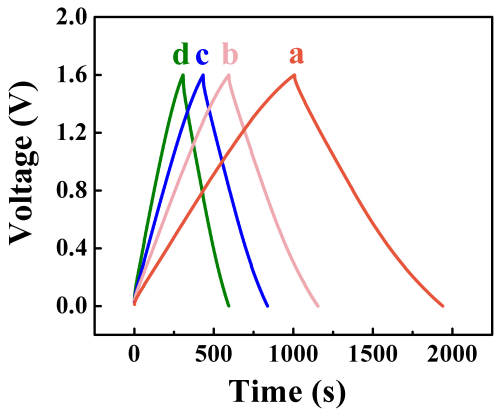

FIGURE 10 | Galvanostatic charge-discharge curves at current densities of (a) 3, (b) 5, (c) 7, (d) 10 mA cm^{-2} for asymmetric supercapacitor cell.

the electrodes was achieved at active mass loading of 40 mg cm^{-2}, which is important for practical applications. It is important to note that low capacitance of negative electrodes is a limiting factor in the development of asymmetric supercapacitor devices. Another difficulty is related to poor cyclic stability of FeOOH electrodes (Shou et al., 2012). Therefore, the high capacitance of the Zn-Fe-DH-MWCNT composites and good cyclic stability are promising for the development of novel supercapacitor devices. It is suggested that more electrochemically negative Zn component allowed for the improved stability of FeOOH active material during cycling. We also suggested that CB facilitates charge transfer (CT) between Zn-Fe-DH and MWCNT and allows for better utilization of charge storage properties of Zn-Fe-DH. The enhanced CT resulted from the catecholate type bonding of CB to Zn-Fe-DH. Catechol-type molecules are widely used as CT mediators in different fields, such as electropolymerization on metal substrates (Tallman et al., 2002; Shi and Zhitomirsky, 2011; Chen and Zhitomirsky, 2013), photovoltaic devices (Wang et al., 2009; Varaganti and Ramakrishna, 2010; Verma et al., 2011) and advanced sensors (Sangeetha and Sriman Narayanan, 2014). In addition, a redox-type mode of the CT mediation can be considered. It is known that CB is an efficient redox-type CT mediator for electrocatalysis (Noorbakhsh et al., 2008), where it is used to transfer electrons between analytes and electrodes. CB shows redox properties in a negative potential range with high electron CT rate constant, excellent reversibility and chemical stability (Noorbakhsh et al., 2008). Therefore, high capacitance of the Zn-Fe-DH-MWCNT electrodes resulted from good dispersion and mixing of the individual components and enhanced CT achieved using CB as a multifunctional additive. It should be noted that direct contribution of CB to the total capacitance is very small due to low amount of CB used and small specific capacitance of this relatively large molecule. The Zn-Fe-DH-MWCNT showed enhanced performance in the negative potential range and outperformed many other candidate materials in the same potential window at high active mass loading in Na_2SO_4 electrolyte. Of particular importance is nearly ideal box shape CV and high areal capacitance. As pointed out above, many hydroxide materials show good capacitive behavior in alkaline electrolytes, such as KOH. The use of environmentally more friendly Na_2SO_4 electrolyte offers benefits for the development of asymmetric devices with enlarged voltage window. Therefore, the Zn-Fe-DH-MWCNT

composites were used as negative electrodes for asymmetric supercapacitor devices.

The fabrication of asymmetric devices with enlarged voltage window requires the development of positive and negative electrodes, operating in partially overlapping voltage windows in the same electrolyte (Zhang Z. et al., 2015; Attias et al., 2017). We found that PPy-MWCNT electrodes are promising as positive electrodes for asymmetric supercapacitor devices in a combination with negative Zn-Fe-DH -MWCNT electrodes. **Figure 7** shows a microstructure of the PPy-MWCNT material, prepared by a chemical polymerization. The material consisted of PPy coated MWCNT. The ECR dispersant for MWCNT acted as an anionic dopant for PPy polymerization and allowed for the fabrication of uniformly coated MWCNT. Such microstructure allowed for enhanced charge transfer between MWCNT and PPy. The CV for the PPy-MWCNT electrode in the 0.5 M Na_2SO_4 electrolyte was of nearly rectangular shape (**Figure 8**) in a voltage window of −0.3 to +0.6 V, which partially overlapped with a voltage window of Zn-Fe-DH -MWCNT negative electrodes. The highest capacitance of 4.2 F cm^{-2} was achieved at a scan rate of 2 mV s^{-1}. The capacitance decreased with increasing scan rate due to electrolyte diffusion limitation in pores. Good electrochemical performance was achieved at a mass loading of 40 mg cm^{-2}, which allowed for a relatively high ratio (0.5) of mass loading to current collector mass.

The Zn-Fe-DH -MWCNT negative electrodes and PPy-MWCNT positive electrodes were used for the fabrication of a novel asymmetric supercapacitor device. Such device showed a nearly rectangular CV in a voltage window of 1.6 V in 0.5 M Na_2SO_4 electrolyte (**Figure 9**). The areal capacitance, calculated from the CV data was found to be 2.2 F cm^{-2} at a scan rate of 2 mV s^{-1}. The device showed triangular shape charge-discharge curves at different current densities in a voltage window of 1.6 V (**Figure 10**).

CONCLUSION

Zn-Fe-DH-MWCNT composite has been developed as a new material for energy storage in negative electrodes of asymmetric supercapacitors. A conceptually new approach is based on the use of CB as a multifunctional additive. We discovered that CB acted as a co-dispersant for Zn-Fe-DH and MWCNT and facilitated their mixing. New strategy was based on the use of CB as charge transfer mediator, which facilitated charge-discharge reactions. The electrodes showed a capacitance of 5.2 F cm^{-2} in a voltage window of −1.0 to −0.2 V vs. SCE and good cyclic stability. A new asymmetric device has been developed, containing Zn-Fe-DH-MWCNT negative electrodes and PPy-MWCNT positive electrodes. Good capacitive behavior of cathode and anode materials was achieved at high active mass of 40 mg cm^{-2} in partially overlapping potential windows. The device showed promising performance in a voltage window of 1.6 V. The capacitance of 2.2 F cm^{-2} was obtained at a scan rate of 2 mV s^{-1}.

DATA AVAILABILITY STATEMENT

The datasets generated for this study are available on request to the corresponding author.

AUTHOR CONTRIBUTIONS

WL conducted synthesis of materials, performed materials characterization and electrochemical testing, and contributed to the writing of the manuscript. IZ contributed to the development of new dispersants, cell design, and writing of the manuscript.

FUNDING

This work was supported by the Natural Sciences and Engineering Research Council of Canada.

ACKNOWLEDGMENTS

We would like to thank the Natural Sciences and Engineering Research Council of Canada for the financial support and Dr. R. Poon for fruitful discussions and technical support. SEM studies were performed at Canadian Centre for Electron Microscopy.

SUPPLEMENTARY MATERIAL

The Supplementary Material for this article can be found online at: https://www.frontiersin.org/articles/10.3389/fmats.2020.00137/full#supplementary-material

REFERENCES

Aghazadeh, M., Dalvand, S., and Hosseinifard, M. (2014). Facile electrochemical synthesis of uniform β-co (oh) 2 nanoplates for high performance supercapacitors. *Ceram. Intern.* 40, 3485–3493.

Ata, M., Liu, Y., and Zhitomirsky, I. (2014). A review of new methods of surface chemical modification, dispersion and electrophoretic deposition of metal oxide particles. *RSC Adv.* 4, 22716–22732.

Ata, M. S., Poon, R., Syed, A. M., Milne, J., and Zhitomirsky, I. (2018). New developments in non-covalent surface modification, dispersion and electrophoretic deposition of carbon nanotubes. *Carbon* 130, 584–598.

Attias, R., Sharon, D., Borenstein, A., Malka, D., Hana, O., Luski, S., et al. (2017). Asymmetric supercapacitors using chemically prepared mno2 as positive electrode materials. *J. Electrochem. Soc.* 164, A2231–A2237.

Brisse, A.-L., Stevens, P., Toussaint, G., Crosnier, O., and Brousse, T. (2018). Ni (oh) 2 and nio based composites: battery type electrode materials for hybrid supercapacitor devices. *Materials* 11:1178. doi: 10.3390/ma11071178

Cesano, F., Cravanzola, S., Brunella, V., Damin, A., and Scarano, D. (2019). From polymer to magnetic porous carbon spheres: combined microscopy, spectroscopy, and porosity studies. *Front. Mater.* 6:84. doi: 10.3389/fmats.2019.00084

Chai, H., Chen, X., Jia, D., Bao, S., and Zhou, W. (2012). Flower-like nio structures: controlled hydrothermal synthesis and electrochemical characteristic. *Mater. Res. Bull.* 47, 3947–3951.

Chen, J., Mosquera-Giraldo, L. I., Ormes, J. D., Higgins, J. D., and Taylor, L. S. (2015). Bile salts as crystallization inhibitors of supersaturated solutions of poorly water-soluble compounds. *Cryst. Growth Des.* 15, 2593–2597.

Chen, M., Liang, X., Wang, F., Xie, D., Pan, G., and Xia, X. (2019). Self-supported vo2 arrays decorated with n-doped carbon as an advanced cathode for lithium-ion storage. *J. Mater. Chem. A* 7, 6644–6650.

Chen, R., Puri, I. K., and Zhitomirsky, I. (2018). High areal capacitance of feooh-carbon nanotube negative electrodes for asymmetric supercapacitors. *Ceram. Intern.* 44, 18007–18015.

Chen, S., and Zhitomirsky, I. (2013). Influence of dopants and carbon nanotubes on polypyrrole electropolymerization and capacitive behavior. *Mater. Lett.* 98, 67–70.

Cheong, M., and Zhitomirsky, I. (2009). Electrophoretic deposition of manganese oxide films. *Surf. Eng.* 25, 346–352.

Dong, M., Wang, Z., Wang, J., Guo, H., Li, X., and Yan, G. (2019). Controlled synthesis of nixcoys4/rgo composites for constructing high-performance asymmetric supercapacitor. *Front. Mater.* 6:176. doi: 10.3389/fmats.2019.000174

Dubal, D., Dhawale, D., Salunkhe, R., Pawar, S., Fulari, V., and Lokhande, C. (2009). A novel chemical synthesis of interlocked cubes of hausmannite mn3o4 thin films for supercapacitor application. *J. Alloys Compounds* 484, 218–221.

Gao, Z., Yang, W., Yan, Y., Wang, J., Ma, J., Zhang, X., et al. (2013). Synthesis and exfoliation of layered α-co (oh) 2 nanosheets and their electrochemical performance for supercapacitors. *Eur. J. Inorgan. Chem.* 2013, 4832–4838.

Hu, M., Ji, X., Lei, L., and Lu, X. (2013). Structural and electrochemical stability of coal layered double hydroxide in alkali solutions. *Electrochim. Acta* 105, 261–274.

Jin, W.-H., Cao, G.-T., and Sun, J.-Y. (2008). Hybrid supercapacitor based on mno2 and columned feooh using li2so4 electrolyte solution. *J. Power Sourc.* 175, 686–691.

Krehula, S., Musiæ, S., Skoko, Z., and Popoviæ, S. (2006). The influence of zn-dopant on the precipitation of α-feooh in highly alkaline media. *J. Alloys Compounds* 420, 260–268.

Lakshmi, V., Ranjusha, R., Vineeth, S., Nair, S. V., and Balakrishnan, A. (2014). Supercapacitors based on microporous β-ni (oh) 2 nanorods. *Coll. Surf. A Physicochem. Eng. Aspects* 457, 462–468.

Li, H., Liu, S., Huang, C., Zhou, Z., Li, Y., and Fang, D. (2011). Characterization and supercapacitor application of coin-like β-nickel hydroxide nanoplates. *Electrochim. Acta* 58, 89–94.

Liu, X., Huang, J., Wei, X., Yuan, C., Liu, T., Cao, D., et al. (2013). Preparation and electrochemical performances of nanostructured coxni1- x (oh) 2 composites for supercapacitors. *J. Power Sourc.* 240, 338–343.

Ma, L., Liu, R., Liu, L., Wang, F., Niu, H., and Huang, Y. (2016). Facile synthesis of ni (oh) 2/graphene/bacterial cellulose paper for large areal mass, mechanically tough and flexible supercapacitor electrodes. *J. Power Sour.* 335, 76–83.

Nasibi, M., Golozar, M. A., and Rashed, G. (2012). Nano iron oxide (fe2o3)/carbon black electrodes for electrochemical capacitors. *Mater. Lett.* 85, 40–43.

Noorbakhsh, A., Salimi, A., and Sharifi, E. (2008). Fabrication of glucose biosensor based on encapsulation of glucose-oxidase on sol-gel composite at the surface of glassy carbon electrode modified with carbon nanotubes and celestine blue. *Electroanalysis* 20, 1788–1797.

Raj, C. J., Kim, B. C., Cho, W.-J., Park, S., Jeong, H. T., Yoo, K., et al. (2015). Rapid hydrothermal synthesis of cobalt oxyhydroxide nanorods for supercapacitor applications. *J. Electroanaly. Chem.* 747, 130–135.

Sangeetha, N., and Sriman Narayanan, S. (2014). Hydrogen peroxide sensor based on carbon nanotubes-poly (celestine blue) nanohybrid modified electrode. *Adv. Mater. Res.* 938, 263–268.

Shi, C., and Zhitomirsky, I. (2010). Electrodeposition and capacitive behavior of films for electrodes of electrochemical supercapacitors. *Nanoscale Res. Lett.* 5:518. doi: 10.1007/s11671-009-9519-z

Shi, C., and Zhitomirsky, I. (2011). Electrodeposition of composite polypyrrole–carbon nanotube films. *Surf. Eng.* 27, 655–661.

Shou, Q., Cheng, J., Zhang, L., Nelson, B. J., and Zhang, X. (2012). Synthesis and characterization of a nanocomposite of goethite nanorods and reduced graphene oxide for electrochemical capacitors. *J. Solid State Chem.* 185, 191–197.

Silva, R., Poon, R., Milne, J., Syed, A., and Zhitomirsky, I. (2018). New developments in liquid-liquid extraction, surface modification and agglomerate-free processing of inorganic particles. *Adv. Coll. Interf. Sci.* 261, 15–27. doi: 10.1016/j.cis.2018.09.005

Su, Y., and Zhitomirsky, I. (2014). Hybrid mno2/carbon nanotube-vn/carbon nanotube supercapacitors. *J. Power Sourc.* 267, 235–242.

Tallman, D., Vang, C., Wallace, G., and Bierwagen, G. (2002). Direct electrodeposition of polypyrrole on aluminum and aluminum alloy by electron transfer mediation. *J. Electrochem. Soc.* 149, C173–C179.

Varaganti, S., and Ramakrishna, G. (2010). Dynamics of interfacial charge transfer emission in small molecule sensitized tio2 nanoparticles: is it localized or delocalized? *J. Phys. Chem. C* 114, 13917–13925.

Verma, S., Ghosh, A., Das, A., and Ghosh, H. N. (2011). Exciton-coupled charge-transfer dynamics in a porphyrin j-aggregate/tio2 complex. *Chem. A Eur. J.* 17, 3458–3464. doi: 10.1002/chem.201002537

Wallar, C., Poon, R., and Zhitomirsky, I. (2017). High areal capacitance of v2o3–carbon nanotube electrodes. *J. Electrochem. Soc.* 164, A3620–A3627.

Wang, G.-L., Xu, J.-J., and Chen, H.-Y. (2009). Dopamine sensitized nanoporous tio2 film on electrodes: photoelectrochemical sensing of nadh under visible irradiation. *Biosens. Bioelectron.* 24, 2494–2498. doi: 10.1016/j.bios.2008.12.031

Wang, J., Song, Y., Li, Z., Liu, Q., Zhou, J., Jing, X., et al. (2010). In situ ni/al layered double hydroxide and its electrochemical capacitance performance. *Energy Fuels* 24, 6463–6467.

Wang, Y., Deen, I., and Zhitomirsky, I. (2011). Electrophoretic deposition of polyacrylic acid and composite films containing nanotubes and oxide particles. *J. Coll. Interf. Sci.* 362, 367–374. doi: 10.1016/j.jcis.2011.07.007

Wang, Y., Yang, W., Zhang, S., Evans, D. G., and Duan, X. (2005). Synthesis and electrochemical characterization of co–al layered double hydroxides. *J. Electrochem. Soc.* 152, A2130–A2137.

Wang, Y.-G., Cheng, L., and Xia, Y.-Y. (2006a). Electrochemical profile of nano-particle coal double hydroxide/active carbon supercapacitor using koh electrolyte solution. *J. Power Sour.* 153, 191–196.

Wang, Y.-G., Yu, L., and Xia, Y.-Y. (2006b). Electrochemical capacitance performance of hybrid supercapacitors based on ni (oh) 2/ carbon nanotube composites and activated carbon. *J. Electrochem. Soc.* 153, A743–A748.

Xi, Y., Wei, G., Li, J., Liu, X., Pang, M., Yang, Y., et al. (2017). Facile synthesis of mno2-ni(oh)2 3d ridge-like porous electrode materials by seed-induce method for high-performance asymmetric supercapacitor. *Electrochim. Acta* 233, 26–35.

Xia, X., Tu, J., Mai, Y., Wang, X., Gu, C., and Zhao, X. (2011). Self-supported hydrothermal synthesized hollow co3o4 nanowire arrays with high supercapacitor capacitance. *J. Mater. Chem.* 21, 9319–9325. doi: 10.34133/2019/8013285

Xu, P., Miao, C., Cheng, K., Ye, K., Yin, J., Cao, D., et al. (2016). Preparation of binder-free porous ultrathin ni (oh) 2 nanoleafs using zno as pore forming agent displaying both high mass loading and excellent electrochemical energy storage performance. *Electrochim. Acta* 216, 499–509.

Zhai, T., Sun, S., Liu, X., Liang, C., Wang, G., and Xia, H. (2018). Achieving insertion-like capacity at ultrahigh rate via tunable surface pseudocapacitance. *Adv. Mater.* 30:1706640.

Zhang, D., Shao, Y., Kong, X., Jiang, M., Lei, D., and Lei, X. (2016). Facile fabrication of large-area hybrid ni-co hydroxide/cu (oh) 2/copper foam composites. *Electrochim. Acta* 218, 294–302.

Zhang, G.-Q., Zhao, Y.-Q., Tao, F., and Li, H.-L. (2006). Electrochemical characteristics and impedance spectroscopy studies of nano-cobalt silicate hydroxide for supercapacitor. *J. Power Sour.* 161, 723–729.

Zhang, Z., Chi, K., Xiao, F., and Wang, S. (2015). Advanced solid-state asymmetric supercapacitors based on 3d graphene/mno 2 and graphene/polypyrrole hybrid architectures. *J. Mater. Chem. A* 3, 12828–12835.

Zhang, Y., Liu, Y., Guo, Y., Yeow, Y. X., Duan, H., Li, H., et al. (2015). In situ preparation of flower-like α-ni (oh) 2 and nio from nickel formate with excellent capacitive properties as electrode materials for supercapacitors. *Mater. Chem. Phys.* 151, 160–166.

Zhou, F., Liu, Q., Gu, J., Zhang, W., and Zhang, D. (2015). Microwave-assisted anchoring of flowerlike co (oh) 2 nanosheets on activated carbon to prepare hybrid electrodes for high-rate electrochemical capacitors. *Electrochim. Acta* 170, 328–336.

Conflict of Interest: The authors declare that the research was conducted in the absence of any commercial or financial relationships that could be construed as a potential conflict of interest.